

Generative Adversarial Network Using Perturbed Convolutions

Seung Park, Yoon-Jae Yeo, and Yong-Goo Shin, *Member, IEEE*

Abstract—Despite growing insights into the adversarial learning, it still suffers from instability during the training procedure. To alleviate this problem, this brief presents a novel convolutional layer, called perturbed convolution (PConv), which focuses on achieving two goals simultaneously: penalize the discriminator for training GAN stably and prevent the overfitting problem in the discriminator. PConv generates perturbed features by randomly disturbing an input tensor before performing the convolution operation. This approach is simple but surprisingly effective. First, to reliably classify real and generated samples using the disturbed input tensor, the intermediate layers in the discriminator should learn features having a small local Lipschitz value. Second, due to the disturbed input tensor, the discriminator is difficult to memorize the real images; this makes the discriminator avoid the overfitting problem. To show the generalization ability of the proposed method, we conducted extensive experiments with various loss functions and datasets including CIFAR-10, CelebA-HQ, LSUN, and tiny-ImageNet. Quantitative evaluations demonstrate that PConv significantly improves the performance of GAN and conditional GAN in terms of Frechet inception distance (FID). For instance, the proposed method improves FID scores on the tiny-ImageNet dataset from 58.59 to 50.42.

Index Terms—Generative adversarial network, Perturbed convolutional layer, Adversarial learning, Convolutional layer

I. INTRODUCTION

GENERATIVE adversarial network (GAN) [1] based on deep convolutional neural networks (CNNs) is one of the leading tools in numerous applications including image-to-image translation [2]–[4], image inpainting [5]–[7], and text-to-image translation [8], [9]. Typically, GAN consists of the generator and the discriminator. In the original setting, both networks are simultaneously trained: the generator is trained to generate a new image that is indistinguishable from real images, whereas the discriminator is optimized to differentiate between real and generated images.

However, GAN still has one major problem: instability in the training procedure [10]. Since a goal of GAN training is finding the Nash equilibrium of non-convex game in the continuous and high dimensional parameter space, GAN is substantially more complicated and difficult to train stably compared with neural networks based on the supervised learning [11]. To alleviate this problem, some researchers [12]–

S. Park is with Medical AI Center, Samsung Medical Center, Irwon-ro, Gangnam-gu, Seoul, 06351, Rep. of Korea, (e-mail: seung1.park@sbsri.co.kr).

Y.-J. Yeo is with School of Electrical Engineering Department, Korea University, Anam-dong, Sungbuk-gu, Seoul, 136-713, Rep. of Korea (e-mail: yjyeo@dali.korea.ac.kr).

Y.-G. Shin is with Division of Smart Interdisciplinary Engineering, Hanyang University, Daedeok-Gu, Daejeon, 34430, Rep. of Korea (e-mail: ygshin@hnu.kr, corresponding author).

[15] propose novel network architectures of discriminator and generator. Although these methods successfully generate high-resolution images on challenging datasets such as ImageNet [16], they cannot resolve the fundamental problem that the instability of GAN training.

Instead of modifying the network architecture, many studies [11], [17]–[22] proposed normalization and regularization techniques that penalize the discriminator for mitigating the instability of GAN training. The most widely used normalization technique is spectral normalization [18] in which weight matrices in the discriminator are divided by an approximation of their largest singular value to impose the Lipschitz constraint. As a regularization, Gulrajani *et al.* [17] introduced the gradient regularization called gradient penalty which penalizes the gradient norm of straight lines between real and generated samples. Kodali *et al.* [22] proposed another form of gradient regularization which constrains the magnitude of the gradient as 1 around the real samples. Roth *et al.* [19] presented a stabilizing regularization technique that directly regularizes the squared gradient norm, where the gradient is calculated with respect to the real and generated samples. These normalization and regularization techniques are effective to improve the performance of GAN. However, some researchers [11], [23] pointed out that when both normalization and gradient-based regularization are used together, the performance is either slightly improved or failed to improve.

Recent studies [15], [24] argued that the overfitting problem is another reason for the instability of the GAN training. As mentioned in [24], when the discriminator memorizes all images from a given dataset as training progresses, *i.e.* the overfitting problem occurs, it disrupts the training dynamics and degrades a generated image quality. As observed by Brock *et al.* [15], this severe problem is not only happened on small datasets; the overfitting problem often occurs on large-scale datasets including ImageNet. To alleviate this problem, some researchers [24]–[27] applied data augmentation techniques such as translation, zoom-in/out, and Cutout [28]. These approaches effectively prevent the overfitting problem and improve GAN performance, but there are too many hyperparameters for controlling the data augmentation strength. For instance, the data augmentation using color adjustment, users should empirically determine the range of adjustments for brightness, contrast, and saturation.

Despite extensive ongoing efforts of developing the normalization, regularization, and data augmentation techniques, a fundamental challenge still exists: instability of GAN training and overfitting problem. To the best of our knowledge, there are no previous works that attempt to develop the

convolutional layer for alleviating this problem. In this brief, we propose a new form of the convolutional layer, called perturbed convolution (PConv), which aims at achieving two goals simultaneously: penalize the discriminator for training GAN stably and avoid the overfitting problem in the discriminator. The proposed method produces perturbed features by randomly disturbing an input tensor in advance of performing the convolution operation. The proposed method is simple but surprisingly effective. First, to reliably classify real and generated samples using the disturbed input tensor, the intermediate layers in the discriminator should learn features having a small local Lipschitz value. Second, owing to the disturbed input tensor, the discriminator is difficult to memorize the real images; this makes the discriminator avoid the overfitting problem. More importantly, by replacing the standard convolutional layer with the perturbed-convolutional layer, the proposed method can be applied to existing network architectures without imposing training overhead or computational costs. To demonstrate the generalization ability of the proposed method, we conducted a series of experiments with various datasets including CIFAR-10, CelebA-HQ, LSUN, and tiny-ImageNet. Quantitative evaluations show that the proposed method significantly improves the performance of GAN and conditional GAN in terms of Inception score (IS) and Frechet inception distance (FID).

In summary, our contributions are summarized as follows: First, we propose a novel convolutional layer, *i.e.* PConv, which is easy for applying to the existing GAN without modifying the network architectures. Second, the proposed method significantly boosts the performance of GAN without imposing the training overhead and computational costs. Finally, we conducted extensive ablation studies to demonstrate the generalization ability of the proposed method. In various datasets and experimental settings, GAN with the proposed method shows better performance than GAN with the standard convolutional layer.

II. RELATED WORKS

A. Generative Adversarial Network

In general, GAN [1] consists of two different networks called generator G and discriminator D . Both networks are trained simultaneously, but their goals are different: G is trained to generate a new image that is indistinguishable from real images, whereas D is optimized to differentiate between real and generated images. This relation can be considered as a two-player min-max game where G and D compete with each other. Formally, the G (D) is trained to minimize (maximize) the following objective functions:

$$\begin{aligned} \min_G \max_D & E_{x \sim P_{\text{data}}(x)} [\log D(x)] \\ & + E_{z \sim P_z(z)} [\log(1 - D(G(z)))] \end{aligned} \quad (1)$$

where z and x denote a random noise vector and a real image sampled from the noise $P_z(z)$ and real data distribution $P_{\text{data}}(x)$, respectively. In order to improve the stability of the training process, a significant amount of research has

been done on modifying the equation 1. For instance, Mao *et al.* [29] employed the least square errors to the objective function (LSGAN), whereas Arjovsky *et al.* [30] computed the loss value by measuring the Wasserstein distance between real and generated distributions (WGAN). Another commonly adopted GAN formulation is a hinge-version of adversarial loss [31], which is written as

$$\begin{aligned} L_D = & E_{x \sim P_{\text{data}}(x)} [\max(0, 1 - D(x))] \\ & + E_{z \sim P_z(z)} [\max(0, 1 + D(G(z)))] \end{aligned} \quad (2)$$

$$L_G = -E_{z \sim P_z(z)} [D(G(z))], \quad (3)$$

where L_D and L_G indicate the objective function for the discriminator and generator, respectively. The current widely-used practice is to employ the hinge-version of adversarial loss while enforcing the spectral normalization [18] either only on the discriminator or both on the discriminator and generator.

B. Regularization for GAN

To stabilize the training dynamics, conventional methods usually added the regularization term to the discriminator. As widely adopted regularization techniques, there are Jensen-Shannon regularization [19], gradient penalty [17], adversarial defence regularization [21], [32], and consistency regularization [11]. All of these methods effectively penalize the discriminator for training GAN stably but often require much training overhead. In particular, although the consistency regularization technique requires a smaller training overhead than other methods, it still requires extra computational costs come from feeding an additional image to the discriminator rather than real and generated images. As we will show in Section III, the proposed method only requires small extra overheads caused by additional summation and multiplication. Thus, the proposed method much easy to implement in practice but significantly improves the performance of GAN.

C. Overfitting problem in GAN

To avoid the overfitting problem, deep learning models in various fields usually adopt label-preserving data augmentation techniques such as region masking [28], flipping, rotation, cropping [33], [34], data mixing [35], and local and affine distortion [36]. Recently, some researchers [11], [24]–[27] apply the data augmentation techniques for training GAN. In particular, Zhao *et al.* [24] conducted extensive experiments with various cases and demonstrated that data augmentation techniques is effective to avoid the overfitting problem. However, as mentioned in Section I, data augmentation techniques require many hyper-parameters for controlling the strength, which makes these techniques difficult to implement in practice.

On the other hand, instead of using data augmentation methods, Brock *et al.* [15] applied dropout technique [37] to the last layer in the discriminator for preventing the over-fitting problem. However, they pointed out that traditional dropout

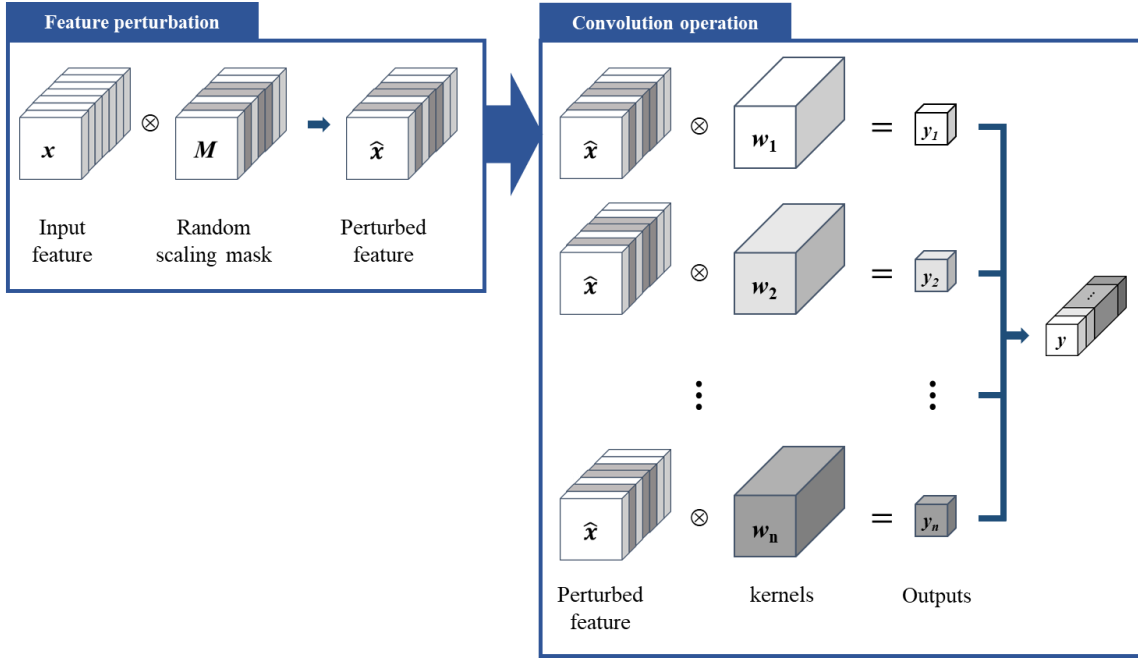


Fig. 1. The overall framework of the proposed method. Unlike the standard convolutional layer, the proposed method disturbed the input tensor before conducting the convolutional operation to produce perturbed features.

strategy could not effective to alleviate the overfitting problem. However, they argued that traditional dropout strategy could alleviate the overfitting problem but it degrades the performance of GAN. In this brief, we also tried to apply the conventional dropout-based approach for preventing the overfitting problem, but showed that performance is drastically degraded when the dropout ratio is increased. The detailed explanations will be described in Section IV-C.

III. PROPOSED METHOD

Before introducing the proposed method, we briefly review the development of GANs: the original version of adversarial loss function (eq. 1) is unstable to train. To address this problem, many regularization terms which impose the Lipschitz constraint to the discriminator have been developed. For instance, the spectral normalization [18] method enforces 1-Lipschitz continuity globally in the discriminator. These approaches commonly aim that the discriminator has a small Lipschitz constant in the intermediate layers. The small Lipschitz constants indicate that the neural network produces similar output values even with the small perturbations in the input. That means, by making the discriminator robust against perturbations, the Lipschitz constants in the intermediate layers become small.

From this point of view, we propose PConv which naturally guides the discriminator to have the small Lipschitz constant. Fig. 1 shows the overall framework of the proposed method. As depicted in Fig. 1, before conducting the convolutional operation, the proposed method randomly disturbs the input tensor by multiplying a random scaling mask in which randomly selected channels have a random constant value $k \in [0, 1]$, others have one. Therefore, PConv with input feature x can be defined as follows:

$$y_i = f_i(x) = (x \otimes M) * w_i, \quad (4)$$

where $f_i(\cdot)$ and w_i indicate the i -th output value and weight, respectively, whereas M is the random scaling mask. Note that the tensor broadcasting is included in Eq. 4 and different random scaling masks are employed to each intermediate layers. This masking operation is simple but meaningful for the discriminator. In order to classify real and generated images even if the input tensor is randomly perturbed, PConv should learn robust features that do not much effect on the next convolutional layer. In other words, to minimize the adversarial loss successfully, $|f_i(x) - f_i(\hat{x})|$ should become a small value, where \hat{x} indicates the perturbed feature, *i.e.* $x \otimes M$. That is to say $f_i(\cdot)$ should have a small local Lipschitz constant; if the Lipschitz constant of $f_i(\cdot)$ is large, the output of the discriminator will change a lot with small perturbations. Therefore, by simply replacing the standard convolutional layer with PConv, it is possible to lead the discriminator to learn robust features with the small Lipschitz constant.

To show the effectiveness of the proposed method, we trained GAN on eight 2D Gaussian mixture models (GMMs) using simple network architectures consisting of multiple fully-connected layers. For a fair comparison, in the discriminator, we only replace the fully-connected layers with the perturbed-f fully-connected layers, *i.e.* PConv being set kernel size as 1. Fig. 2 shows the experimental results. As training progresses, the GAN consisting of standard fully-connected layers suffers from the mode collapse problem, whereas the GAN with the perturbed-f fully-connected layers learns all GMMs successfully. These results indicate that the proposed method is much better than the standard convolutional layer in GAN training. More extensive experiments will be presented

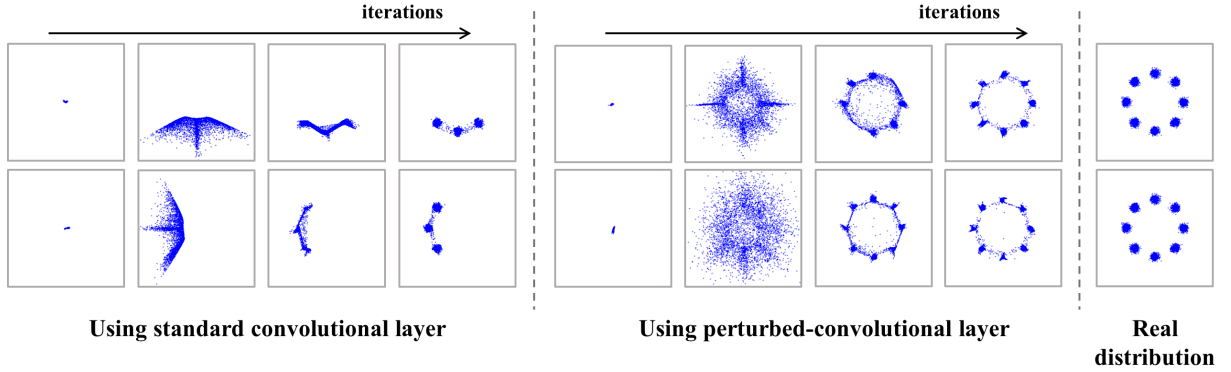


Fig. 2. The illustration of the experimental results on eight 2D Gaussian mixture models. We trained the networks two times to reveal the true trend of the perturbed-convolutional layer module.

```

def PConv(tensor, w, b, Lamda_R):
    # tensor : input features with shape [N, H, W, C]
    # w, b : convolutional kernels and bias
    # Lamda_R : ratio of channels scaled randomly

    # x is a vector consisting of ones
    x = tf.ones_like(tf.reduce_mean(tensor, axis=(1, 2), keep_dims=True))
    rand_scale = tf.random.uniform((1, 1, 1, 1), minval=0.0, maxval=1.0)

    # Rescaling x which is up-scaled due to 'tf.nn.dropout' function
    ch_one = tf.nn.dropout(x, rate=Lamda_R) * (1 - drop_prob)
    ch_perturbed = (1 - ch_one) * rand_scale

    M = ch_one + ch_perturbed

    return tf.nn.conv2d(tensor * M, filters=w) + b

```

Fig. 3. Python code of perturbed-convolutional layer based on *TensorFlow*.

in the next section. The detailed implementation code for PConv based on *Tensorflow* is described in Algorithm 1. We only need to specify how to build the random scaling mask before performing the convolutional layer. In other words, the proposed method does not increase training overhead; the only extra computational cost comes from multiplying the different random scaling masks to the input tensors in the mini-batch.

Indeed, one may anticipate that the proposed method is similar to the conventional spatial-dropout (SDrop) method [38], which dropouts the randomly selected channels of the input feature. However, there is a major difference between the proposed method and the conventional one: the existence of the random scaling value k . More specifically, SDrop sets the randomly selected channels as 0, whereas the proposed method scales down the features in those channels by multiplying k . This small difference has a large effect on GAN training. To prove the theoretical validity of this assumption, we will show an example. Let us consider \mathbf{x} as an n -dimensional vector, *i.e.* $\mathbf{x} = \{x_1, \dots, x_n\}^T$ where $x_1 \geq \dots \geq x_n$, and the output of the convolutional layer, *i.e.* y , is a single scalar value. That means the convolutional layer contains a single kernel vector $\mathbf{w} = \{w_1, w_2, \dots, w_n\}^T$. When SDrop method is applied to this convolutional layer, the variation range of y , Δy , can be defined as follows:

$$\mathbf{d}_{\min}^T \mathbf{w} \leq \Delta y \leq \mathbf{d}_{\max}^T \mathbf{w}, \quad (5)$$

where \mathbf{d}_{\min} and \mathbf{d}_{\max} are perturbed vectors which produce the minimum and maximum changes when they are projected onto \mathbf{w} , respectively. For instance, when n is 10 and dropout ratio (λ_R) is set to 0.1, $\mathbf{d}_{\min} = \{x_1, \dots, x_9, 0\}$ and $\mathbf{d}_{\max} = \{0, x_2, \dots, x_{10}\}$. In contrast, when applying PConv, the range of Δy becomes

$$0 \leq \Delta y \leq \mathbf{d}_{\max}^T \mathbf{w}, \quad (6)$$

since \mathbf{d}_{\min} is zero when random scaling value is 1. As described in Eqs. 5 and 6, the PConv can produce the output without variations, but SDrop is not. In other words, since there is at least $\mathbf{d}_{\min}^T \mathbf{w}$ variant in the features, the discriminator using SDrop is difficult to produce the decision boundaries that guide the generator well. In addition, when the dropout ratio becomes large, the minimum boundary of Δy is increased in the case of SDrop, but PConv is not changed. Therefore, the proposed method is less sensitive to the dropout ratio compared with SDrop. The comparison of GAN performance between SDrop and the proposed method will be introduced in Section IV-C.

IV. EXPERIMENTS

A. Implementation details

In order to evaluate the effectiveness of the proposed method, we conducted extensive experiments using the CIFAR-10 [39], LSUN [40], CelebA [41], CelebA-HQ [12], [41], and tiny-ImageNet [42], [43] datasets. The CIFAR-10 and LSUN datasets consist of 10 classes, whereas tiny-ImageNet, which is a subset of ImageNet [42], is composed of 200 classes. Among a large number of images in LSUN, we randomly selected 30,000 images for each class; we employed 300,000 images for training. In addition, we resized the images from the CelebA and LSUN datasets as 64×64 pixels, whereas tiny-ImageNet as 128×128 pixels. For evaluating the performance when generating the high-resolution image, we employed CelebA-HQ by resizing images into 256×256

TABLE I
DETAILED ARCHITECTURES OF GENERATOR ACCORDING TO THE IMAGE RESOLUTION.

32 × 32 resolution	64 × 64 resolution	128 × 128 resolution	256 × 256 resolution	512 × 512 resolution
$z \in \mathbb{R}^{128} \sim N(0, I)$	$z \in \mathbb{R}^{128} \sim N(0, I)$	$z \in \mathbb{R}^{128} \sim N(0, I)$	$z \in \mathbb{R}^{256} \sim N(0, I)$	$z \in \mathbb{R}^{256} \sim N(0, I)$
FC, 4 × 4 × 256	FC, 4 × 4 × 512			
ResBlock, up, 256	ResBlock, up, 512	ResBlock, up, 512	ResBlock, up, 512	ResBlock, up, 512
ResBlock, up, 256				
ResBlock, up, 256	ResBlock, up, 128	ResBlock, up, 128	ResBlock, up, 128	ResBlock, up, 128
BN, ReLU				
3 × 3 conv, Tanh				

TABLE II
DETAILED ARCHITECTURES OF DISCRIMINATOR ACCORDING TO THE IMAGE RESOLUTION.

32 × 32 resolution	64 × 64 resolution	128 × 128 resolution	256 × 256 resolution	512 × 512 resolution
RGB image	RGB image	RGB image	RGB image	RGB image
ResBlock, down, 128	ResBlock, down, 64	ResBlock, down, 32	ResBlock, down, 32	ResBlock, down, 16
ResBlock, down, 128	ResBlock, down, 128	ResBlock, down, 64	ResBlock, down, 64	ResBlock, down, 32
ResBlock, 128	ResBlock, down, 256	ResBlock, down, 128	ResBlock, down, 128	ResBlock, down, 64
ResBlock, 128	ResBlock, down, 512	ResBlock, down, 256	ResBlock, down, 256	ResBlock, down, 128
ReLU	ReLU	ReLU	ReLU	ReLU
Global sum pooling	Global sum pooling	Global sum pooling	Global sum pooling	Global sum pooling
Dense, 1	Dense, 1	Dense, 1	Dense, 1	Dense, 1

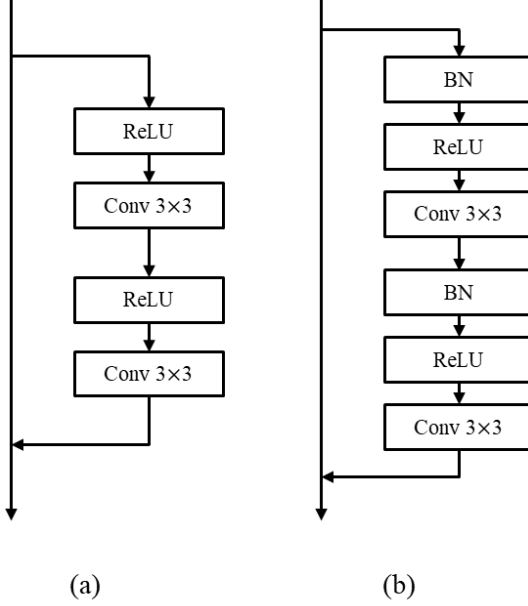


Fig. 4. Detailed architectures of the ResBlock used in our experiments. (a) ResBlock of the discriminator, (b) ResBlock of the generator.

and 512 × 512 resolutions. As an adversarial objective function, we adopted the *hinge*-version loss in Eqs. 2 and 3.

Since all parameters in the generator and the discriminator including PConv can be differentiated, we performed an optimization using the Adam optimizer [44], which is a stochastic

optimization method with adaptive estimation of moments. We set the parameters of Adam optimizer, *i.e.* β_1 and β_2 , to 0 and 0.9, respectively, and set the learning rate to 0.0002. During the last 50,000 iterations of training, we decrease the learning rate linearly. Like the conventional methods [17], [18], [30], [45], we updated the discriminator five times using different mini-batches when the generator is updated once. For the CIFAR-10, CelebA, and LSUN datasets, we set a batch size as 64 and trained the generator for 50k, 100k, and 100k iterations, respectively. In addition, for the CelebA-HQ and tiny-ImageNet, we trained the network 100k and 450k iterations with 16 and 32 batch sizes, respectively. It is worth noting that we trained the generator with a batch size twice as large as when training the discriminator. For instance, on the CIFAR-10 dataset, we trained the discriminator with a batch size of 64, whereas the generator was trained with a batch size of 128. The proposed method contains a single hyper-parameter λ_R which determines how many channels are scaled randomly during the training procedure. It will be described in Section IV-C how we determined λ_R value.

In this brief, we employed the generator and discriminator architectures consisting of multiple residual blocks [46] as our baseline models [18], [45], [47]. The detailed generator and discriminator architectures are presented in Tables I and II, where ResBlock is depicted in Fig. 4. In the discriminator, we employed the spectral normalization [18] for all layers. For the discriminator, the down-sampling (average-pooling) is performed after the second convolutional layer, whereas the generator up-samples the feature maps using a nearest-

TABLE III
COMPARISON OF THE PROPOSED METHOD WITH SDROP ON CIFAR-10 IN TERMS OF FID.

Method		$\lambda_R = 0.1$	$\lambda_R = 0.2$	$\lambda_R = 0.3$
SDrop	trial 1	12.73	16.96	88.21
	trial 2	13.31	16.47	85.96
	trial 3	12.99	16.20	85.30
Average		13.01 ± 0.29	16.55 ± 0.38	85.30 ± 3.29
SDrop*	trial 1	13.07	16.13	94.79
	trial 2	12.65	16.14	73.56
	trial 3	14.53	16.04	85.86
Average		13.42 ± 0.99	16.10 ± 0.05	84.74 ± 10.66
Proposed	trial 1	12.31	12.62	14.31
	trial 2	12.58	12.77	14.43
	trial 3	12.89	12.45	13.90
Average		12.59 ± 0.29	12.61 ± 0.16	14.21 ± 0.28

TABLE IV
COMPARISON OF FID SCORES IN DIFFERENT SIZES OF DATASETS ON CIFAR-10.

Dataset size		Conv	PConv
Full	trial 1	13.21	12.31
	trial 2	13.44	12.58
	trial 3	13.57	12.89
Average		13.41 ± 0.18	12.59 ± 0.29
Half	trial 1	17.54	14.44
	trial 2	17.47	13.50
	trial 3	18.21	14.07
Average		17.74 ± 0.41	14.00 ± 0.47
Quarter	trial 1	25.79	17.84
	trial 2	27.25	19.45
	trial 3	24.74	17.89
Average		25.93 ± 1.26	18.39 ± 0.92

neighbor interpolation prior to the first convolution layer.

B. Evaluation metric

In order to evaluate how ‘realistic’ each generated image is, we employed the most popular assessments, called Frechet inception distance (FID) [48], which measures the visual appearance and diversity of the generated images. The FID measures the Wasserstein distance between the distribution of the real images, P_R , and that of the generated ones, P_G , in the feature space obtained via the Inception model [49], which is defined as follows:

$$\text{FID}(p, q) = \|\mu_p - \mu_q\|_2^2 + \text{trace}(C_p + C_q - 2(C_p C_q)^{1/2}), \quad (7)$$

where $\{\mu_p, C_p\}, \{\mu_q, C_q\}$ are the mean and covariance of the samples with distribution P_R and P_G , respectively. Lower FID scores indicate better quality of the generated images. In our experiments, we randomly generated 50,000 images for CIFAR-10, LSUN, CelebA, and tiny-ImageNet and 30,000 images for Celeb-HQ.

C. Quantitative comparison

Before evaluating the performance of the proposed method on various datasets, we first present ablation studies on the

TABLE V
COMPARISON OF FID SCORES IN DIFFERENT LOSS SETTINGS ON CIFAR-10.

Loss function		Conv	PConv
CE [1]	trial 1	16.72	14.10
	trial 2	17.81	14.14
	trial 3	16.65	13.80
Average		17.06 ± 0.65	14.02 ± 0.19
LSGAN [29]	trial 1	19.72	19.43
	trial 2	19.60	18.82
	trial 3	20.81	19.45
Average		20.04 ± 0.66	19.24 ± 0.36
Hinge [31]	trial 1	13.21	12.31
	trial 2	13.44	12.58
	trial 3	13.57	12.89
Average		13.41 ± 0.18	12.59 ± 0.29

CIFAR-10 dataset. In order to show that performance improvement is not caused by lucky weight initialization, we trained the network three times from scratch. First, we discuss the difference between the proposed method and SDrop [38]. As shown in Table III, SDrop shows poor performance compared with the proposed method. In particular, the proposed method shows stable performance even with an increasing value of λ_R . In contrast, the performance of SDrop is drastically degraded when λ_R value becomes large. To make our results more reliable, we conducted additional experiments that randomly change λ_R of SDrop during the training procedure. That means we checked whether SDrop shows fine performance when \mathbf{d}_{\min} in Eq. 5 is zero. In order to statistically match the dropout ratio with other experiments, we randomly change λ_R in the range $[\lambda_R - 0.1, \lambda_R + 0.1]$. For instance, when λ_R is set to 0.1, the statistical dropout ratio is 0.1 while \mathbf{d}_{\min} becomes zero. As described in Table III, SDrop with random dropout ratio (we denoted it as SDrop*), shows a similar trend with SDrop. Because, although \mathbf{d}_{\min} becomes zero, SDrop* still converts the randomly selected channels as zero, which disturbs the adversarial learning. As mentioned in [15], these results demonstrate that the dropout-based techniques are not appropriate for GAN. Thus, in the field of GAN, it is better to apply PConv instead of dropout techniques for improving the performance. Since the performance of PConv is not significantly different when $\lambda_R = 0.1$ and $\lambda_R = 0.2$, in the rest of this brief, we conducted other experiments by setting λ_R as 0.1.

We investigated whether the proposed method would alleviate the discriminator overfitting problem. Since the overfitting problem usually occurs when the number of real images is small. we trained the network using only the half or quarter number of images on the CIFAR-10 dataset. As shown in Table IV, the performance of the network using the standard convolutional layer is degraded when the number of training images becomes smaller. The discriminator cannot guide the generator well since it classifies real and generated samples by memorizing the real images, *i.e.* the overfitting problem. In contrast, the network trained with the proposed method achieves better performance since PConv could restrict the discriminator from memorizing real images. Therefore, we expect that the proposed method is able to alleviate the

TABLE VI

COMPARISON OF THE PROPOSED METHOD WITH THE STANDARD CONVOLUTIONAL LAYER ON CIFAR-10, CELEBA, LSUN, AND TINY-IMAGENET IN TERMS OF FID.

Dataset	Unconditional GAN				Conditional GAN			
	Conv		PConv		Conv		PConv	
CIFAR-10	trial 1	13.21	trial 1	12.31	trial 1	13.36	trial 1	12.55
	trial 2	13.44	trial 2	12.58	trial 2	13.76	trial 2	11.64
	trial 3	13.57	trial 3	12.89	trial 3	14.46	trial 3	12.27
	Average	13.41 ± 0.18	Average	12.59 ± 0.29	Average	13.86 ± 0.56	Average	12.15 ± 0.47
CelebA	trial 1	6.10	trial 1	5.50	trial 1	-	trial 1	-
	trial 2	5.90	trial 2	5.44	trial 2	-	trial 2	-
	trial 3	5.98	trial 3	6.12	trial 3	-	trial 3	-
	Average	6.00 ± 0.10	Average	5.69 ± 0.38	Average	-	Average	-
LSUN	trial 1	19.10	trial 1	16.58	trial 1	17.32	trial 1	16.91
	trial 2	19.40	trial 2	15.83	trial 2	17.42	trial 2	16.73
	trial 3	19.50	trial 3	16.84	trial 3	18.78	trial 3	16.24
	Average	19.33 ± 0.21	Average	16.42 ± 0.52	Average	17.87 ± 0.78	Average	16.63 ± 0.34
tiny-ImageNet	trial 1	55.44	trial 1	51.46	trial 1	34.53	trial 1	34.06
	trial 2	60.66	trial 2	50.90	trial 2	34.98	trial 2	32.93
	trial 3	59.68	trial 3	48.90	trial 3	34.59	trial 3	33.61
	Average	58.59 ± 2.77	Average	50.42 ± 1.34	Average	34.70 ± 0.24	Average	33.53 ± 0.57

overfitting problem in the field of the GAN. Furthermore, to demonstrate the generalization ability of the proposed method, we trained the networks using various adversarial loss functions. In this brief, we conducted additional experiments using two different loss functions: the loss function based on the cross-entropy (CE) theorem (Eq. 1) and loss function proposed in the least square GAN (LSGAN) paper [29]. As shown in Table V, even with various loss functions, the proposed method still has superior performance compared with the standard convolutional layer. These results reveal that the proposed method can be easily applied to the GAN without considering experimental settings such as the adversarial loss function.

Extensive experimental results on various datasets are summarized in Table VI. First, in the unconditional GAN scheme, the proposed method shows superior performance than the standard convolutional layer. In particular, on LSUN and tiny-ImageNet datasets containing complex images that are difficult to generate, the proposed method significantly improves the generator performance. These results indicate that even with spectral normalization, the discriminator using the standard convolution layer often suffers from the training instability problem. In contrast, by simply replacing the standard convolutional layer with the proposed method, we can train the generator stably as well as achieve higher performance. However, the proposed method shows slightly better performance than the standard convolutional layer on the CelebA dataset. Because low-resolution face images are easy to generate with conventional techniques; it is difficult to further enhance the performance. When generating the high-resolution face images, however, the proposed method shows significantly superior performance compared with the conventional method. We will show the experimental results related to high-resolution images later.

We conducted additional experiments to validate the effectiveness of the proposed method in the conditional GAN scheme. We employed the same baseline model with the experiments of GAN, but replaced the BN in the generator with the conditional batch normalization layer [50] and

TABLE VII
COMPARISON OF THE PROPOSED METHOD WITH THE STANDARD CONVOLUTIONAL LAYER ON CELEBA-HQ IN TERMS OF FID.

Resolution	Conv		PConv
	trial 1	trial 2	trial 3
256 × 256	23.32	21.98	15.63
	21.98	23.13	-
	Average	22.81 ± 0.72	14.96 ± 0.80
512 × 512	28.11	29.32	20.34
	29.32	28.18	-
	Average	28.54 ± 0.68	20.84 ± 2.87

added the conditional projection layer in the discriminator; this conditional-baseline model is equivalent to the model in [45] which leads the cGAN scheme. Similar to the trend of experimental results of unconditional GAN, as described in Table VI, the proposed method achieves better performance than the conventional method [45]. These results demonstrate that the proposed method can be applied to the conditional GAN scheme to boost the performance.

To show the effectiveness of the proposed method for generating the high-resolution image, we conducted additional experiments using the CelebA-HQ dataset. In our experiments, we trained the networks to generate 256×256 and 512×512 images. As shown in Table VII, the proposed method shows significantly low FID scores compared with the standard convolutional layer. In addition, as depicted in Fig. 5, the proposed method allows the generator to produce visually pleasing images. These results show that the proposed method is effective to generate high-resolution images with high quality. Indeed, this brief does not intend to design an optimal generator and discriminator architectures for PConv; there could be another structure that leads to better performance and generates more high-quality images. In contrast, we care more about whether it is possible to improve the performance of GAN by simply replacing the standard convolutions with PConvs.



Fig. 5. Examples of the generated images with 512×512 and 256×256 resolutions on the Celeb-HQ dataset.

V. CONCLUSION

In this brief, we have introduced a straightforward method for boosting the performance of GAN. By replacing the standard convolutional layer with PConv, the discriminator effectively guides the generator during the training procedure, which results in enhancing the ability of the generator. One of the main advantages of the proposed method is that it can be readily integrated with the existing discriminator architectures. Moreover, our experiments reveal that, without imposing the training overhead, the discriminator with PConv significantly improves the performance of the baseline models. In addition, we demonstrate the generalization ability of the proposed method in various aspects through high-resolution image generation and many-sided ablation studies. It is expected that the proposed method will be applicable to various applications based on GAN.

REFERENCES

- [1] I. Goodfellow, J. Pouget-Abadie, M. Mirza, B. Xu, D. Warde-Farley, S. Ozair, A. Courville, and Y. Bengio, “Generative adversarial nets,” in *Advances in neural information processing systems*, 2014, pp. 2672–2680. [1](#) [2](#) [6](#)
- [2] P. Isola, J.-Y. Zhu, T. Zhou, and A. A. Efros, “Image-to-image translation with conditional adversarial networks,” in *Proceedings of the IEEE conference on computer vision and pattern recognition*, 2017, pp. 1125–1134. [1](#)
- [3] Y. Choi, M. Choi, M. Kim, J.-W. Ha, S. Kim, and J. Choo, “Stargan: Unified generative adversarial networks for multi-domain image-to-image translation,” in *Proceedings of the IEEE Conference on Computer Vision and Pattern Recognition*, 2018, pp. 8789–8797. [1](#)
- [4] J.-Y. Zhu, T. Park, P. Isola, and A. A. Efros, “Unpaired image-to-image translation using cycle-consistent adversarial networks,” in *Proceedings of the IEEE international conference on computer vision*, 2017, pp. 2223–2232. [1](#)
- [5] J. Yu, Z. Lin, J. Yang, X. Shen, X. Lu, and T. S. Huang, “Free-form image inpainting with gated convolution,” *arXiv preprint arXiv:1806.03589*, 2018. [1](#)
- [6] Y.-G. Shin, M.-C. Sagong, Y.-J. Yeo, S.-W. Kim, and S.-J. Ko, “Pepsi++: fast and lightweight network for image inpainting,” *IEEE Transactions on Neural Networks and Learning Systems*, 2020. [1](#)
- [7] M.-c. Sagong, Y.-g. Shin, S.-w. Kim, S. Park, and S.-j. Ko, “Pepsi: Fast image inpainting with parallel decoding network,” in *Proceedings of the IEEE Conference on Computer Vision and Pattern Recognition*, 2019, pp. 11360–11368. [1](#)
- [8] S. Reed, Z. Akata, X. Yan, L. Logeswaran, B. Schiele, and H. Lee, “Generative adversarial text to image synthesis,” *arXiv preprint arXiv:1605.05396*, 2016. [1](#)
- [9] S. Hong, D. Yang, J. Choi, and H. Lee, “Inferring semantic layout for hierarchical text-to-image synthesis,” in *Proceedings of the IEEE Conference on Computer Vision and Pattern Recognition*, 2018, pp. 7986–7994. [1](#)
- [10] T. Salimans, I. Goodfellow, W. Zaremba, V. Cheung, A. Radford, and X. Chen, “Improved techniques for training gans,” in *Advances in neural information processing systems*, 2016, pp. 2234–2242. [1](#)
- [11] H. Zhang, Z. Zhang, A. Odena, and H. Lee, “Consistency regularization for generative adversarial networks,” *arXiv preprint arXiv:1910.12027*, 2019. [1](#) [2](#)
- [12] T. Karras, T. Aila, S. Laine, and J. Lehtinen, “Progressive growing of gans for improved quality, stability, and variation,” *arXiv preprint arXiv:1710.10196*, 2017. [1](#) [4](#)
- [13] H. Zhang, I. Goodfellow, D. Metaxas, and A. Odena, “Self-attention generative adversarial networks,” *arXiv preprint arXiv:1805.08318*, 2018. [1](#)
- [14] H. Zhang, T. Xu, H. Li, S. Zhang, X. Wang, X. Huang, and D. N. Metaxas, “Stackgan++: Realistic image synthesis with stacked generative adversarial networks,” *IEEE transactions on pattern analysis and machine intelligence*, vol. 41, no. 8, pp. 1947–1962, 2018. [1](#)
- [15] A. Brock, J. Donahue, and K. Simonyan, “Large scale gan training for high fidelity natural image synthesis,” *arXiv preprint arXiv:1809.11096*, 2018. [1](#) [2](#) [6](#)
- [16] A. Krizhevsky, I. Sutskever, and G. E. Hinton, “Imagenet classification with deep convolutional neural networks,” in *Advances in neural information processing systems*, 2012, pp. 1097–1105. [1](#)
- [17] I. Gulrajani, F. Ahmed, M. Arjovsky, V. Dumoulin, and A. C. Courville, “Improved training of wasserstein gans,” in *Advances in neural information processing systems*, 2017, pp. 5767–5777. [1](#) [2](#) [5](#)
- [18] T. Miyato, T. Kataoka, M. Koyama, and Y. Yoshida, “Spectral normalization for generative adversarial networks,” *arXiv preprint arXiv:1802.05957*, 2018. [1](#) [2](#) [3](#) [5](#)
- [19] K. Roth, A. Lucchi, S. Nowozin, and T. Hofmann, “Stabilizing training of generative adversarial networks through regularization,” in *Advances in neural information processing systems*, 2017, pp. 2018–2028. [1](#) [2](#)
- [20] L. Mescheder, A. Geiger, and S. Nowozin, “Which training methods for gans do actually converge?” *arXiv preprint arXiv:1801.04406*, 2018. [1](#)
- [21] B. Zhou and P. Krähenbühl, “Don’t let your discriminator be fooled,” in *International Conference on Learning Representations*, 2018. [1](#) [2](#)

[22] N. Kodali, J. Abernethy, J. Hays, and Z. Kira, "On convergence and stability of gans," *arXiv preprint arXiv:1705.07215*, 2017. [1](#)

[23] K. Kurach, M. Lučić, X. Zhai, M. Michalski, and S. Gelly, "A large-scale study on regularization and normalization in gans," in *International Conference on Machine Learning*. PMLR, 2019, pp. 3581–3590. [1](#)

[24] S. Zhao, Z. Liu, J. Lin, J.-Y. Zhu, and S. Han, "Differentiable augmentation for data-efficient gan training," *Advances in Neural Information Processing Systems*, vol. 33, 2020. [1, 2](#)

[25] T. Karras, M. Aittala, J. Hellsten, S. Laine, J. Lehtinen, and T. Aila, "Training generative adversarial networks with limited data," *Advances in Neural Information Processing Systems*, vol. 33, 2020. [1, 2](#)

[26] N.-T. Tran, V.-H. Tran, N.-B. Nguyen, T.-K. Nguyen, and N.-M. Cheung, "Towards good practices for data augmentation in gan training," *arXiv preprint arXiv:2006.05338*, 2020. [1, 2](#)

[27] Z. Zhao, Z. Zhang, T. Chen, S. Singh, and H. Zhang, "Image augmentations for gan training," *arXiv preprint arXiv:2006.02595*, 2020. [1, 2](#)

[28] T. DeVries and G. W. Taylor, "Improved regularization of convolutional neural networks with cutout," *arXiv preprint arXiv:1708.04552*, 2017. [1, 2](#)

[29] X. Mao, Q. Li, H. Xie, R. Y. Lau, Z. Wang, and S. Paul Smolley, "Least squares generative adversarial networks," in *Proceedings of the IEEE international conference on computer vision*, 2017, pp. 2794–2802. [2, 6, 7](#)

[30] M. Arjovsky, S. Chintala, and L. Bottou, "Wasserstein gan," *arXiv preprint arXiv:1701.07875*, 2017. [2, 5](#)

[31] J. H. Lim and J. C. Ye, "Geometric gan," *arXiv preprint arXiv:1705.02894*, 2017. [2, 6](#)

[32] X. Liu and C.-J. Hsieh, "Rob-gan: Generator, discriminator, and adversarial attacker," in *Proceedings of the IEEE conference on computer vision and pattern recognition*, 2019, pp. 11 234–11 243. [2](#)

[33] A. Krizhevsky, I. Sutskever, and G. E. Hinton, "Imagenet classification with deep convolutional neural networks," *Communications of the ACM*, vol. 60, no. 6, pp. 84–90, 2017. [2](#)

[34] L. Wan, M. Zeiler, S. Zhang, Y. Le Cun, and R. Fergus, "Regularization of neural networks using dropconnect," in *International conference on machine learning*, 2013, pp. 1058–1066. [2](#)

[35] H. Zhang, M. Cisse, Y. N. Dauphin, and D. Lopez-Paz, "mixup: Beyond empirical risk minimization," *arXiv preprint arXiv:1710.09412*, 2017. [2](#)

[36] P. Y. Simard, D. Steinkraus, J. C. Platt *et al.*, "Best practices for convolutional neural networks applied to visual document analysis." in *Icdar*, vol. 3, no. 2003, 2003. [2](#)

[37] N. Srivastava, G. Hinton, A. Krizhevsky, I. Sutskever, and R. Salakhutdinov, "Dropout: a simple way to prevent neural networks from overfitting," *The journal of machine learning research*, vol. 15, no. 1, pp. 1929–1958, 2014. [2](#)

[38] J. Tompson, R. Goroshin, A. Jain, Y. LeCun, and C. Bregler, "Efficient object localization using convolutional networks," in *Proceedings of the IEEE conference on computer vision and pattern recognition*, 2015, pp. 648–656. [4, 6](#)

[39] A. Torralba, R. Fergus, and W. T. Freeman, "80 million tiny images: A large data set for nonparametric object and scene recognition," *IEEE transactions on pattern analysis and machine intelligence*, vol. 30, no. 11, pp. 1958–1970, 2008. [4](#)

[40] F. Yu, Y. Zhang, S. Song, A. Seff, and J. Xiao, "Lsun: Construction of a large-scale image dataset using deep learning with humans in the loop," *arXiv preprint arXiv:1506.03365*, 2015. [4](#)

[41] Z. Liu, P. Luo, X. Wang, and X. Tang, "Deep learning face attributes in the wild," in *Proceedings of the IEEE International Conference on Computer Vision*, 2015, pp. 3730–3738. [4](#)

[42] J. Deng, W. Dong, R. Socher, L.-J. Li, K. Li, and L. Fei-Fei, "Imagenet: A large-scale hierarchical image database," in *2009 IEEE conference on computer vision and pattern recognition*. Ieee, 2009, pp. 248–255. [4](#)

[43] L. Yao and J. Miller, "Tiny imagenet classification with convolutional neural networks," *CS 231N*, 2015. [4](#)

[44] D. P. Kingma and J. Ba, "Adam: A method for stochastic optimization," *arXiv preprint arXiv:1412.6980*, 2014. [5](#)

[45] T. Miyato and M. Koyama, "cgans with projection discriminator," *arXiv preprint arXiv:1802.05637*, 2018. [5, 7](#)

[46] K. He, X. Zhang, S. Ren, and J. Sun, "Deep residual learning for image recognition," in *Proceedings of the IEEE conference on computer vision and pattern recognition*, 2016, pp. 770–778. [5](#)

[47] Y. J. Yeo, Y. G. Shin, S. Park, and S. J. Ko, "Simple yet effective way for improving the performance of gan," *IEEE Transactions on Neural Networks and Learning Systems*, 2021. [5](#)

[48] M. Heusel, H. Ramsauer, T. Unterthiner, B. Nessler, and S. Hochreiter, "Gans trained by a two time-scale update rule converge to a local nash equilibrium," in *Advances in Neural Information Processing Systems*, 2017, pp. 6626–6637. [6](#)

[49] C. Szegedy, V. Vanhoucke, S. Ioffe, J. Shlens, and Z. Wojna, "Rethinking the inception architecture for computer vision," in *Proceedings of the IEEE conference on computer vision and pattern recognition*, 2016, pp. 2818–2826. [6](#)

[50] V. Dumoulin, J. Shlens, and M. Kudlur, "A learned representation for artistic style," *Proc. of ICLR*, vol. 2, 2017. [7](#)